

SUPPLEMENTAL INFORMATION

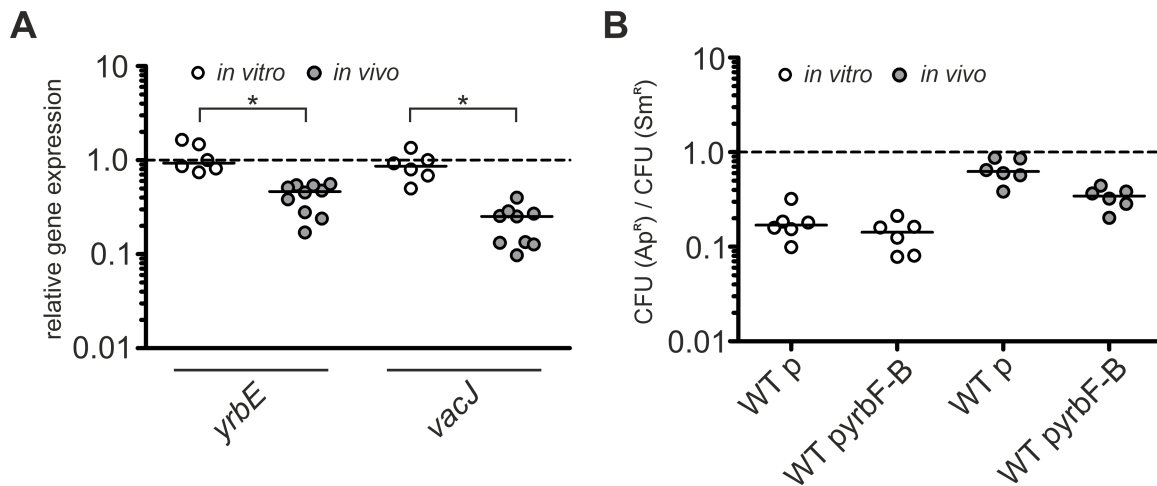


Figure S1. *In vivo* repression of *yrbE* and *vacJ* as well as plasmid maintenance of p and pyrBF-B in absence of antibiotic selection. Related to Figure 1.

(A) Relative expression levels of *yrbE* and *vacJ* were determined by quantitative real time PCR *in vitro* (n = 6) during growth in LB broth (open circles) and *in vivo* (n = 10 for *yrbE* and n = 9 for *vacJ*) during intestinal colonization (22 h post-infection, grey circles).

(B) Plasmid maintenance of the empty pMMB67EH vector (p, Ap^R) and the *yrb* operon expression vector (pyrBF-B, Ap^R) in *V. cholerae* is indicated as the ratio of CFU (Ap^R) / CFU (Sm^R) after 22 h growth in LB broth (open circles) and *in vitro* during intestinal colonization (22 h post-infection, grey circles). A ratio of 1 (dashed line) indicates optimal plasmid stability. Horizontal bars indicate the median of each data set (n = 6).

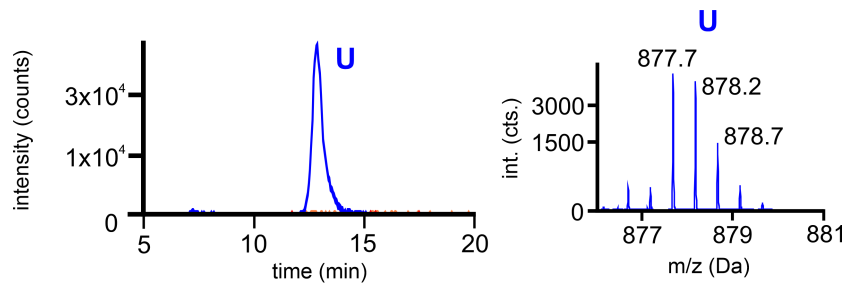


Figure S2. Mass spectrometry analysis of lipid A extracted from the $\Delta almG$ mutant. Related to Figure 3.

Lipid A extracted after the M9 to M9^{ToxR \uparrow /Alm \uparrow} transition from $\Delta almG$ after 8 h was analyzed. Comparable to figure 3 the left graph shows the extracted ion chromatogram of m/z 877.7 (U, representing unmodified lipid A) in blue, m/z 906.2 (M1, representing mono-glycinated lipid A) in orange, and m/z 934.7 (M2, representing di-glycinated lipid A) in red. Only the unmodified lipid A species at m/z 877.7 could be detected, the mono- and di-glycinated lipid A species were below limit of detection. In addition, the high-resolution mass spectrum of the unmodified doubly charged lipid A species with its isotope pattern is displayed in the right graph.

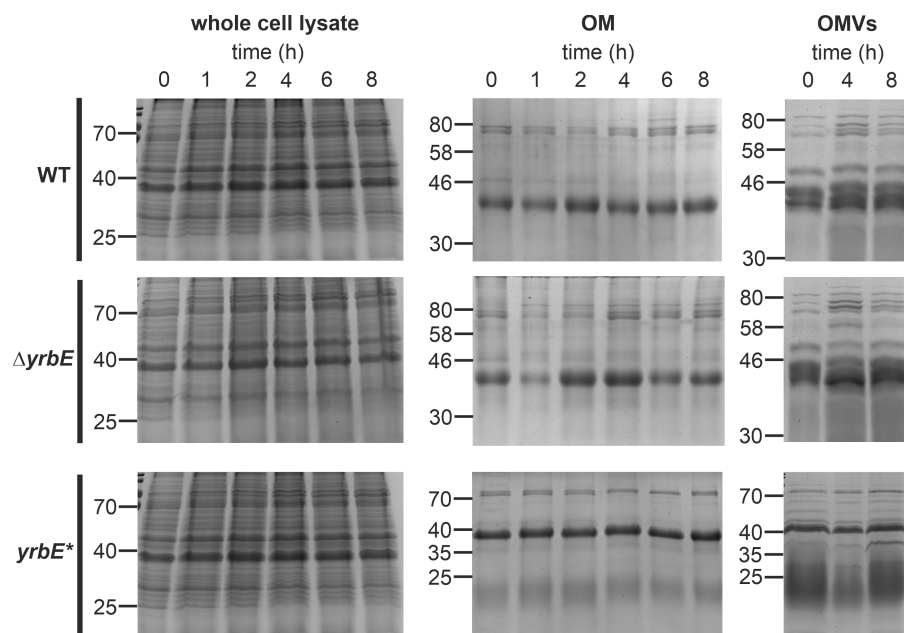


Figure S3. Coomassie-stained gels of whole cell lysates, OM preparations and isolated OMVs derived from WT, $\Delta yrbE$ and $yrbE^*$. Related to Figure 4.

Shown are Coomassie-stained gels loaded with cell equivalents of whole cell lysates or protein equivalents (5 μ g) of OM preparations and OMVs from WT, $\Delta yrbE$ and $yrbE^*$. Samples were taken at time points 0, 1, 2, 4, 6 and 8 h for whole cell lysates and OM as well as 0, 4 and 8 h for OMVs after transition from M9 to M9^{ToxR \uparrow} . Molecular mass standards are indicated on the left using either Prestained Protein Marker Broad Range (New England Biolab) or PageRulerTM Prestained Protein Ladder 10 - 180 kDa (Thermo Fisher).

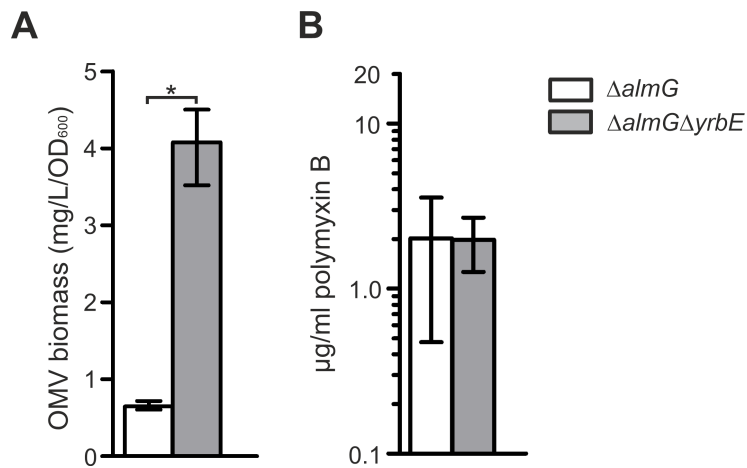


Figure S4. OMV production and minimal inhibitory concentrations (MIC) of polymyxin B (PMB) determined for $\Delta almG$ and $\Delta almG\Delta yrbE$. Related to Figure 5.

(A) Quantification of OMV biomass (Bradford) prepared from equivalent OD₆₀₀ units of $\Delta almG$ and $\Delta almG\Delta yrbE$ after 8 h cultivation in minimal media M9^{ToxR \uparrow} . Data is presented as the median with interquartile range (n = 6; * $P < 0.05$).

(B) Shown are minimal inhibitory concentrations (MIC) of polymyxin B (PMB) for the $\Delta almG$ (n = 12) and $\Delta almG\Delta yrbE$ mutants (n = 15) along a transition from M9 to M9^{ToxR \uparrow /Alm \uparrow} [(di)glycine-modified lipid A activating conditions using sub-MIC PMB concentrations (0.3 μg/ml)]. Bacteria were allowed to adapt for 2 h after transition into the fresh medium before additional PMB was added in diverse concentrations to determine the MIC. Results are presented as mean \pm SD (* $P < 0.05$).

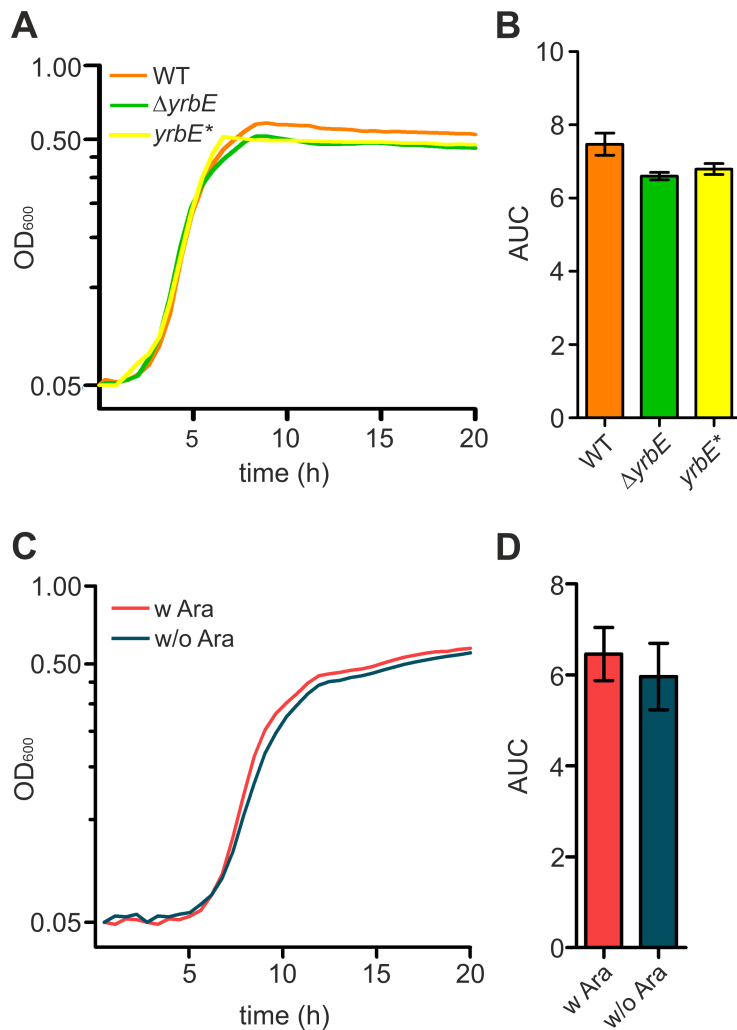


Figure S5. Hyper- or hypo-vesiculation by deletion of *yrbE* or overexpression of *yrbF-B* does not affect growth in minimal media $M9^{ToxR^\uparrow}$. Related to Figure 5.

Shown are growth curves (A, C) and the retrieved area under curve (AUC) values (B, D) for the *V. cholerae* WT, $\Delta yrbE$ and the complementation strain $yrbE^*$ (A, B) shifted from M9 to $M9^{ToxR^\uparrow}$ or the arabinose-inducible strain $yrbF-B^{pARA}$ shifted from M9 to $M9^{ToxR^\uparrow}$ with (w) or without (w/o) arabinose (Ara) (C, D). Data is presented as mean values \pm SD with the following number of biological replicates: $n = 4$ for WT and $\Delta yrbE$ as well as $n = 8$ for $yrbE^*$, $yrbF-B^{pARA}$ w Ara and $yrbF-B^{pARA}$ w/o Ara, respectively.

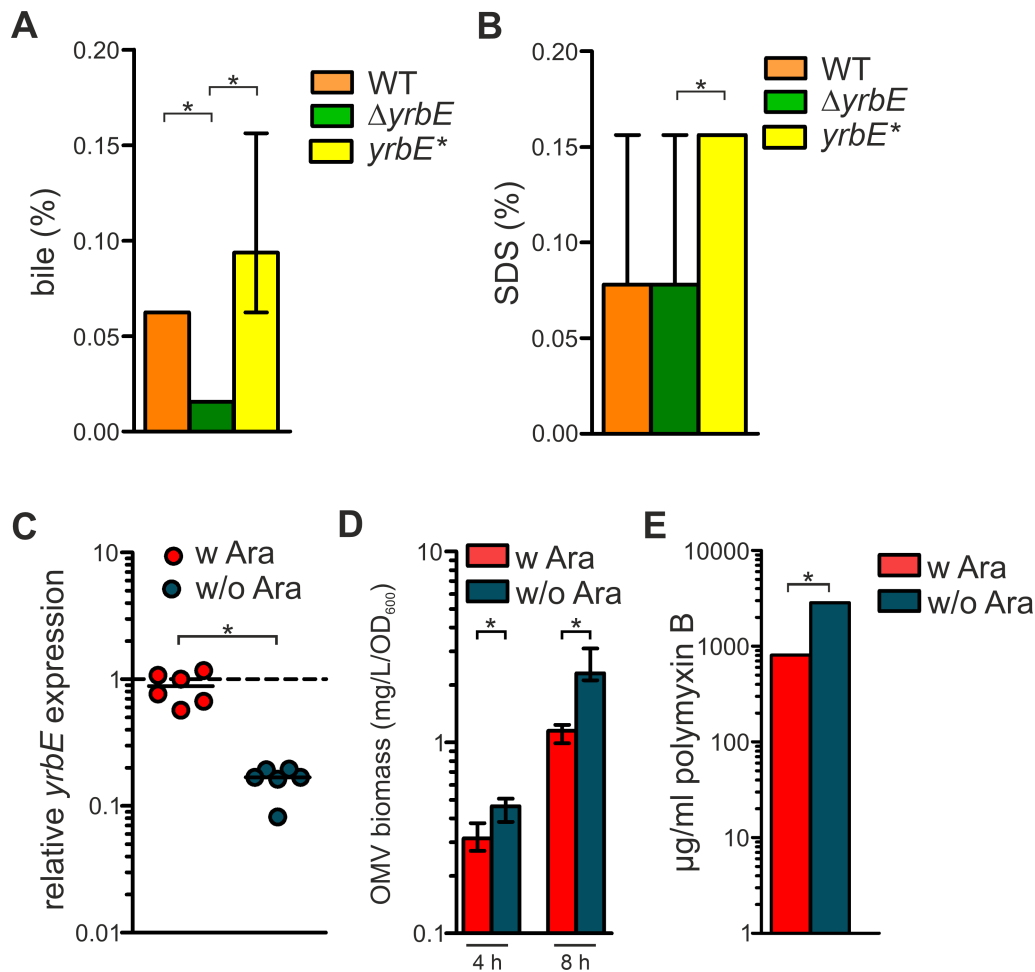


Figure S6. Minimal inhibitory concentrations (MIC) of antimicrobial substances and OMV production for various *V. cholerae* strains used in this study. Related to Figure 5.

(A and B) Shown are minimal inhibitory concentrations (MIC) of bile (A) and SDS (B) for WT, $\Delta yrbE$ and the complementation strain $yrbE^*$ grown in M9. Data is presented as the median with interquartile range ($*P < 0.05$) with the following number of biological replicates: MIC of bile for WT ($n = 22$), for $\Delta yrbE$ ($n = 8$) and for $yrbE^*$ ($n = 18$) as well as $n = 12$ for the MIC of SDS for all strains tested.

(C) Relative expression levels of $yrbE$ in the arabinose-inducible $yrbF$ - B variant were determined by quantitative real time PCR *in vitro* during growth in M9^{ToxR \uparrow} with (w) or without (w/o) arabinose (Ara) ($n = 6$; $*P < 0.05$).

(D) Quantification of OMV biomass (Bradford) prepared from equivalent OD₆₀₀ units of the arabinose-inducible $yrbF$ - B variant. Values were obtained after 4 and 8 h cultivation in minimal

media M9^{ToxR[↑]} with (w) or without (w/o) arabinose (Ara). Data is presented as the median with interquartile range (n = 6; **P* < 0.05).

(E) Shown are the minimal inhibitory concentrations (MIC) of the arabinose-inducible strain *yrbF-B^{pARA}* against polymyxin B (PMB) along a transition from M9 to M9^{ToxR[↑]/Alm[↑]} [(di)glycine-modified lipid A activating conditions using sub-MIC PMB concentrations (3 µg/ml)] with (w) or without (w/o) arabinose (Ara). Bacteria were allowed to adapt for 2 h after transition into the fresh medium before additional PMB was added in diverse concentrations to determine the MIC. Results are presented as mean ± SD (n = 6; **P* < 0.05).

Table S1. List of oligonucleotides used in this study, related to STAR Methods

Oligonucleotides	Source
almG_XbaI_1 AATTCTAGAGGCAAACAGTTAGTGAAGGG	This paper
almG_BamHI_2 TATGGATCCTTTTTTCCGACTTATCGGCTTA	This paper
almG_BamHI_3 AAAGGATCCAAGCAATTCGGTGTATCTAAGA	This paper
almG_SacI_4 AATGAGCTCTCCACAATAAGTTGTGCCAAAG	This paper
lacZ_XbaI_1 TATCTAGAATGTACGCCGTAGAGCAAAG	This paper
lacZ_BamHI_2 TAGGATCCATGGCGAGTCACTTGGCTAA	This paper
lacZ_SphI_3 ATGCATGCGTGTGGAATGTGACGAT	This paper
lacZ_SacI_4 ATGAGCTCTTATTGTGGGGATGACCTTTAAAG	This paper
araC_BamHI_1 AAAGGATCCAGACACTTTTGTACGCGTTTT	This paper
araC_SphI_2 ATTGCATGCTTATGACAACTGACGGCTAC	This paper
yrb_SacI_1 AAAGAGCTCGCGATATTGGCAATGTTTGAAC	This paper
yrb_SphI_2 AAAGCATGCGATAAGGATAATTAATTGGAATC	This paper
yrb_EcoRI_3 AAAGAATTCTCAGGATGTCGACCTAACAG	This paper
yrb_XbaI_4 TTTTCTAGAGATTAAGGTTACGGATCAGTTC	This paper
para_SphI_1 AAAGCATGCAAAGCCATGACAAAAACGCG	This paper
para_EcoRI_2 GAATTCGCTAGCCCCAAAAAAC	This paper
almG_pGPphoA_SacI TTGAGCTCGTTAACCTCAGGTTTATTTTATTT	This paper
almG_pGPphoA_KpnI ATTGGTACCTTACTTAAAACGCCGATAAAGC	This paper
yrb_operon_SacI_1 TTTGAGCTCTTTCAGGATGTCGACCTAA	This paper
yrb_operon_XbaI_2 AAATCTAGACTATCCACAATTCACCTCTGC	This paper
VC2519_XbaI_up_fw AAATCTAGACTTAGTCAACCATCAAAAATT	(Roier et al., 2016)
VC2519_XmaI_down_rv AAACCCGGGCTCCGCCACATCTTCACGTT	This paper
comp_yrbE*_1 GTTGCATGTTAATTCCTAAACATCAATGCGG	This paper
comp_yrbE*_2 TTTGGAATTAACATGCAACAAACACGAAAAATTG	This paper